

Diffusion of Aromatic Hydrocarbons in *n*-Alkanes and Cyclohexanes

Bruce A. Kowert,* Nhan C. Dang, Kurtis T. Sobush, and Louis G. Seele III

Department of Chemistry, Saint Louis University, St. Louis, Missouri 63103

Received: August 22, 2000; In Final Form: November 27, 2000

The translational diffusion constants, D , of biphenyl, diphenylacetylene, diphenylbutadiyne, anthracene, pyrene, rubrene, perylene, and coronene have been determined in the *n*-alkanes using capillary flow techniques. Pyrene and rubrene were also studied in cyclohexane and several of its derivatives. The solutes showed varying degrees of deviation from the Stokes–Einstein (SE) relation ($D = k_B T / 6\pi\eta r$); the values of the hydrodynamic radius r decrease as the viscosity η increases. The data can be fitted to $D/T = A/\eta^p$ with $p < 1$ ($p = 1$ for the SE relation). The values of p increase as the solute size increases. In the *n*-alkanes, they range from $p = 0.718 \pm 0.004$ for biphenyl to $p = 0.943 \pm 0.014$ for rubrene; the largest value ($p = 0.982 \pm 0.019$) is found for rubrene in the cyclohexanes. The D values have been compared with reorientational results and molecular dynamics calculations; they have also been fitted to the Doolittle–Cohen–Turnbull free volume equation. A correlation between the p values and the results of the free volume analyses is discussed.

Introduction

The determination of the translational diffusion constant, D , of symmetric aromatic hydrocarbons in the *n*-alkanes and cyclohexanes is of interest for several reasons. Because of their relatively weak solute–solvent interactions, these systems are well suited for checking theories of diffusion and the predictions of molecular dynamics (MD) calculations. Aromatic hydrocarbons such as pyrene and anthracene have also been used as probes of molecular motion in polymers,¹ glasses,² and biochemical systems.³ Data in the *n*-alkanes would serve as benchmarks in the discussion of translational diffusion in these more complex environments.

The rotational motion of aromatic solutes in the *n*-alkanes has been the subject of several studies.^{4–7} The reorientational correlation times, τ_θ , have been discussed in terms of the Stokes–Einstein–Debye (SED) relation^{4,7,8}

$$\tau_\theta = (V/k_B)(\eta/T) \quad (1)$$

where V is the effective hydrodynamic volume of the solute (which is understood to include frictional and shape effects^{4,7}), k_B is Boltzmann's constant, T is the absolute temperature, and η is the viscosity. Deviations from eq 1 have been found^{5,6} in constant-temperature experiments using C_5 – C_{16} (C_i is used for n - C_iH_{2i+2}).

The D values of aromatic hydrocarbons have not been studied as extensively. Their viscosity and temperature dependence can be compared with that predicted by the Stokes–Einstein (SE) relation^{9–11}

$$D = k_B T / (f\pi\eta r) \quad (2)$$

where r is the solute's hydrodynamic radius and $f = 6$ and 4 for the stick and slip limits, respectively. In this paper we report the translational diffusion constants for several aromatic hydrocarbons (Figures 1 and 2) in multiple *n*-alkanes and cyclohexanes. The D values, determined using microcapillary

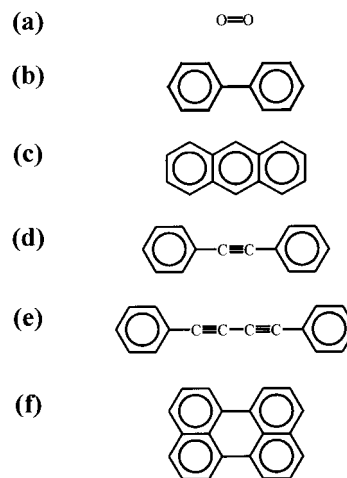


Figure 1. Structures of (a) dioxygen, (b) biphenyl, (c) anthracene, (d) diphenylacetylene, (e) diphenylbutadiyne, and (f) perylene.

techniques^{9,10} and Taylor–Aris dispersion theory,^{12,13} show deviations from the SE relation, which decrease as the solute size increases.

The deviations were quantified using^{9–11,14,15}

$$D/T = A_{SE}/\eta^p \quad (3)$$

where p and A_{SE} are constants; $p = 1$ for the SE limit. Our earlier studies^{9,10} of O_2 showed clear deviations from the SE relation; i.e., $p = 0.553 \pm 0.009$ in the relatively extended *n*-alkanes C_6 – C_{16} and 0.632 ± 0.017 in a series of cycloalkanes.¹⁰ The small p values are due to the weak solute–solvent interactions and the small solute/solvent size ratios; the more globular shape of the cycloalkanes was mentioned as a possible reason for their larger p value. The hydrodynamic SE limit should be approached as the solute/solvent size ratio increases. We first considered biphenyl in C_6 – C_{16} and anthracene, diphenylacetylene, and diphenylbutadiyne in the odd *n*-alkanes C_7 – C_{15} . As expected, these solutes have smaller deviations from SE behavior than O_2 ; p varies from 0.718 ± 0.004 for biphenyl to 0.797 ± 0.009 for diphenylbutadiyne.

* To whom correspondence should be addressed. Phone: (314) 977-2837. Fax: (314) 977-2521. E-mail: kowertba@slu.edu.

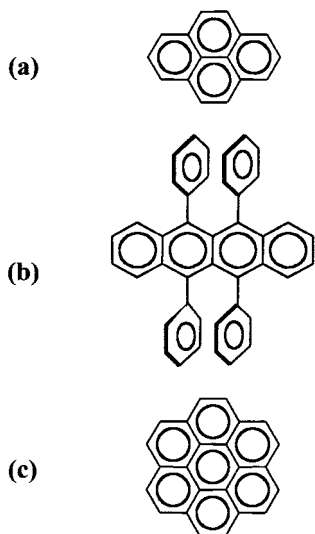


Figure 2. Structures of (a) pyrene, (b) rubrene, and (c) coronene.

We then studied perylene in C_6 – C_{15} , coronene in the even n -alkanes C_6 – C_{14} , pyrene in C_6 – C_{16} , and rubrene in the odd n -alkanes C_7 – C_{15} , all of which were found to have larger p values than biphenyl and its counterparts. The D values for rubrene showed only small deviations from SE behavior ($p = 0.943 \pm 0.014$). Rubrene clearly has strong solute–solvent interactions; the four phenyl groups attached to its tetracene nucleus cause it to experience close to the full viscous drag of the solvent. As was the case for O_2 , the p values for rubrene and pyrene in the cyclic solvents (cyclohexane, dicyclohexyl, methylcyclohexane, and n -butylcyclohexane) are larger than in the n -alkanes.

The D values for our aromatic solutes in the n -alkanes can also be fitted to the Doolittle–Cohen–Turnbull^{16,17} free volume equation. A correlation between the p values and the results of the free volume analyses is discussed in terms of the sizes of the diffusing species. We have also compared our diffusion constants with the predictions of MD calculations and with the τ_θ data for our own and similar probes in the n -alkanes.

Experimental Section

Biphenyl, diphenylacetylene, diphenylbutadiyne, perylene, coronene, pyrene, and rubrene were from Aldrich Chemical Co.; anthracene was from Fisher. They, as well as the solvents, were used as received. With the exception of C_6 (Fisher Optima), C_7 (Fisher HPLC grade), and C_8 (Sigma, 99+%), the n -alkanes (all 99+%) were obtained from Aldrich as were methylcyclohexane (99+%), n -butylcyclohexane (99+%), and dicyclohexyl (99%). Cyclohexane (HPLC grade) was obtained from Fisher. The viscosities for the n -alkanes, cyclohexane, and methylcyclohexane are from ref 18; those for n -butylcyclohexane and dicyclohexyl are from ref 19.

The pure solvent was drawn through a fused silica microcapillary (Polymicro Technology, 77 μm i.d.) for several hours by reduced pressure. The reduced pressure was then broken; the capillary was dipped in a dilute solution (3–5 mM, except for pyrene and coronene, which were ~ 0.14 mM) containing the same solvent and the solute of interest for a load time t . The capillary was then returned to the pure solvent as the reduced pressure and data acquisition were reset and started, respectively. The solute elution profiles were recorded using UV detection; the detector, data acquisition system, and calculation of D from the profiles are described in refs 9 and 10. The load time was decreased, introducing progressively

TABLE 1: Detection Wavelengths and Fit Parameters for Eq 2

solute	solvent	λ_{max}	p	$-(\log A_{\text{SE}})$
biphenyl ^a	n -alkanes	240	0.718 ± 0.004	8.782 ± 0.008
anthracene ^b	n -alkanes	236	0.749 ± 0.011	8.884 ± 0.022
diphenylacetylene ^b	n -alkanes	268	0.752 ± 0.011	8.929 ± 0.021
diphenylbutadiyne ^b	n -alkanes	268	0.797 ± 0.009	9.085 ± 0.020
pyrene ^a	n -alkanes	236	0.805 ± 0.006	9.060 ± 0.012
pyrene ^c	cyclohexanes	236	0.857 ± 0.019	9.192 ± 0.037
perylene ^d	n -alkanes	254	0.822 ± 0.007	9.162 ± 0.013
coronene ^e	n -alkanes	304	0.858 ± 0.009	9.300 ± 0.018
rubrene ^b	n -alkanes	300	0.943 ± 0.014	9.710 ± 0.030
rubrene ^c	cyclohexanes	300	0.982 ± 0.019	9.821 ± 0.036
O_2 ^{a,f}	n -alkanes	190	0.553 ± 0.009	7.878 ± 0.018
O_2 ^{e,f,g}	cycloalkanes	190	0.632 ± 0.017	8.074 ± 0.030

^a In C_6 – C_{16} . ^b In the odd n -alkanes C_7 – C_{15} . ^c In cyclohexane, dicyclohexyl, methylcyclohexane, and n -butylcyclohexane. ^d In C_6 – C_{15} . ^e In the even n -alkanes C_6 – C_{14} . ^f From ref 10. ^g In *cis*- and *trans*-decalin.

smaller amounts of solute into the solvent flow; the results were extrapolated to “zero load time”, corresponding to infinite dilution. The detection wavelengths for all solutes (Table 1) were determined with a Hewlett-Packard model 8452A diode array spectrophotometer. The elution profiles were obtained at room temperature, which was essentially constant during the determination of all D values, varying by no more than ± 0.5 °C during the 2–4 h needed for an individual determination. The temperatures for most of the determinations were between 20 and 25 °C and ranged from 17 to 25.5 °C.

Special precautions were taken for anthracene; the profiles in its first solvent (C_9) were considerably less intense the second day it was studied. The solution had been prepared and stored in a clear volumetric flask with the lights on (as they were while profiles were being obtained). These results are consistent with the formation of the photodimer of anthracene,²⁰ which has a much weaker absorption at the detection wavelength (236 nm) used for anthracene. A second solution was prepared with the lights off and stored in a volumetric flask covered with aluminum foil. The lights were left off while profiles were obtained; their intensities and D values were unchanged from the first day to the second. Similar precautions were taken for rubrene; the D values became $\sim 10\%$ larger as its first solution’s orange color (in C_9) lightened to yellow after 3 days; the autosenitized photooxidation of rubrene gives a colorless product and can be avoided by using dimmed light.²¹ When a second solution was prepared and studied in the dark, its color and D values were the same as on the first day of the first solution. None of these problems were encountered for the other solutes.

Results and Discussion

SE Comparison and Modification. The D values for our solutes in the n -alkanes and cyclohexanes were fitted to eq 3. Plots of $\log(D/T)$ vs $\log \eta$ for O_2 , biphenyl, pyrene, and rubrene in the n -alkanes are shown in Figure 3; the values of $\log A_{\text{SE}}$ and p are given in Table 1 (as are those for O_2).

All but one of the solute–solvent systems have $p < 1$. The p values tend to increase (the deviations from the SE relation decrease) as the solute size increases. In an effort to relate p to the sizes of our solutes, the half-lengths of their molecular axes, R_i , were determined from structural data^{22–30} and van der Waals radii.³¹ They, with the n -alkane p values, are given in Table 2 and show several trends. The p values of biphenyl (0.718 ± 0.004), diphenylacetylene (0.752 ± 0.011), and diphenylbutadiyne (0.797 ± 0.009) increase as the length of the longest molecular

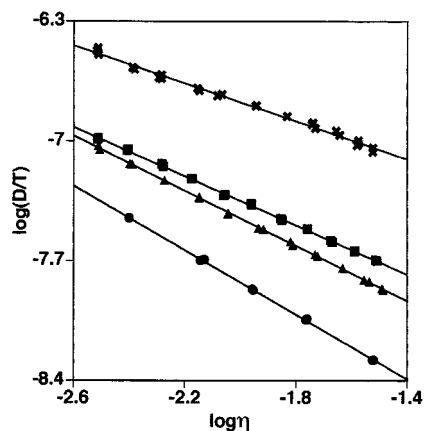


Figure 3. Fits of the diffusion constants for O₂ (×), biphenyl (■), pyrene (▲), and rubrene (●) in the *n*-alkanes to $D/T = A/\eta^p$ (η in P).

TABLE 2: Solute Radii from Structural Data and van der Waals Radii^a

solute	R_x , Å	R_y , Å	R_z , Å	R , Å	p^b
O ₂ ^c	2.10	1.50	1.50	1.68	0.553
biphenyl ^d	5.67	2.94	2.19	3.32	0.718
anthracene ^e	5.62	3.52	1.77	3.27	0.749
diphenylacetylene ^e	6.95	3.19	1.77	3.40	0.752
diphenylbutadiyne ^e	8.23	3.18	1.77	3.59	0.797
pyrene ^e	5.62	4.41	1.77	3.53	0.805
perylene ^e	5.65	4.57	1.77	3.57	0.822
coronene ^e	5.65	5.65	1.77	3.84	0.858
rubrene ^f	6.82	7.83	2.13	4.85	0.943

^a For right-handed axes. ^b In the *n*-alkanes. ^c The *x* axis is collinear with the internuclear axis. ^d The *x* axis is collinear with the bond connecting the two phenyl rings, and the *y* axis bisects the 42° angle between the phenyl rings. ^e The *z* axis is perpendicular to the molecular plane, and the *x* axis is collinear with the longest in-plane axis. ^f The *z* axis is perpendicular to the plane of the tetracene nucleus, and the *x* axis is collinear with the longest axis of the tetracene nucleus.

symmetry axis increases. Anthracene is about the same length but wider than biphenyl; its p value (0.749 ± 0.011) is greater than that of biphenyl and essentially the same as that for diphenylacetylene. Pyrene may be considered to be an enlarged biphenyl; the addition of the two additional six-membered rings raises its p value to 0.805 ± 0.006 . Rubrene has the largest p value (0.943 ± 0.014) in the *n*-alkanes; the four phenyl substituents are “oars in the water” and clearly impede its diffusion. The values of p in the *n*-alkanes are plotted vs $R = (R_x R_y R_z)^{1/3}$ in Figure 4. The data show an approximately linear relationship. Chen, Davis, and Evans,¹⁵ however, used $p = -a/R + b$ for several monatomic and polyatomic solutes in the *n*-alkanes. The inset of Figure 4 shows such a plot for the aromatic hydrocarbon solutes; the agreement is reasonably good (O₂, well off the line, is not included).

The solute radius r (from eq 2) decreases as the *n*-alkane chain length increases and is usually smaller than R because of the deviations from the SE relation. Table 3 shows the stick-limit values of r in C₇ and C₁₅. Only rubrene in C₇ has r (5.15 Å) slightly larger than R (4.85 Å). The solvent-dependent change in r decreases as p increases (and the SE limit is approached). For O₂, $\Delta r = 100[r(C_7) - r(C_{15})]/r(C_7) = 57\%$; for rubrene $\Delta r = 10\%$.

The p values for pyrene (0.857 ± 0.019) and rubrene (0.982 ± 0.019) in the cycloalkanes are larger than in the *n*-alkanes, but the difference $\Delta p = p_{\text{cycloalkanes}} - p_{\text{n-alkanes}}$ decreases as the solute size increases; $\Delta p = 0.079 \pm 0.019$, 0.052 ± 0.020 , and 0.039 ± 0.024 for O₂, pyrene, and rubrene, respectively. While the values of Δp are small compared to the

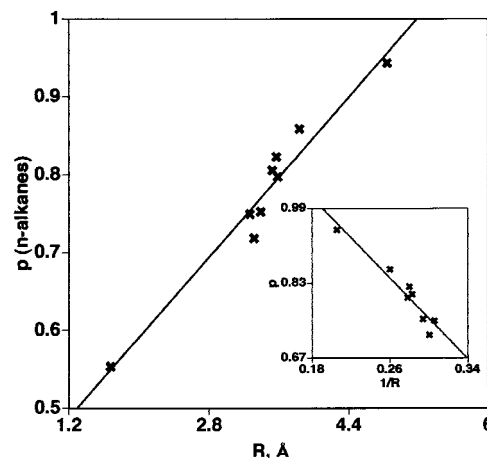


Figure 4. p values in the *n*-alkanes vs R . Data are from Table 2; the fit line is $p = 0.1284R + 0.3345$. Inset: p values for our aromatic hydrocarbon solutes vs $1/R$. The fit line is $p = -2.158/R + 1.401$.

TABLE 3: Stick-Limit Values of r in C₇ and C₁₅^a

solute	p	$r(C_7)$, Å	$r(C_{15})$, Å	Δr , % ^b	R , Å
O ₂	0.553	0.663	0.285	57	1.68
biphenyl	0.718	2.03	1.25	38	3.32
anthracene	0.749	2.26	1.41	38	3.27
diphenylacetylene	0.752	2.46	1.54	37	3.40
diphenylbutadiyne	0.797	2.76	1.88	32	3.59
pyrene	0.805	2.48	1.72	31	3.53
perylene	0.822	2.85	2.04	28	3.57
coronene	0.858	3.21	2.46	23	3.84
rubrene	0.943	5.15	4.63	10	4.85

^a Values of r are calculated using eq 2 and D values at 25 °C obtained from fits to eq 3. ^b $\Delta r = 100[r(C_7) - r(C_{15})]/r(C_7)$.

TABLE 4: Comparison with Literature D Values

solute	solvent	temp, K	$10^5 D$, cm ² s ⁻¹	
			literature	this work ^a
biphenyl	C ₁₄	298.2	0.792 ± 0.009^b	0.790 ± 0.016
biphenyl	C ₇	303.2	2.72 ± 0.12^c	2.81 ± 0.05
biphenyl	C ₈	303.2	2.28 ± 0.03^c	2.31 ± 0.04
anthracene	C ₇	303.2	2.71 ± 0.03^c	2.65 ± 0.06
anthracene	C ₈	303.2	2.16 ± 0.03^c	2.16 ± 0.05
anthracene	C ₆	298.2	3.16 ± 0.04^d	3.02 ± 0.07
anthracene	C ₈	298.2	2.01 ± 0.03^d	2.04 ± 0.05
anthracene	C ₁₆	298.2	0.540 ± 0.010^d	0.535 ± 0.016
pyrene	C ₆	298.2	2.93 ± 0.04^d	2.80 ± 0.07

^a From fits to eq 3. ^b Reference 33. ^c Reference 34. ^d Reference 35.

individual values of $p_{\text{cycloalkanes}}$ and $p_{\text{n-alkanes}}$, the trend shown by these differences is reasonable; the shape of the two types of solvents becomes less important as the solute size increases. The larger solutes have nearly the same interactions with both the *n*-alkanes and cycloalkanes; the smaller solutes can diffuse between the relatively extended *n*-alkanes (MD calculations of C₁₆ give an end-to-end distance of 14.5 Å³²) without experiencing the solvent viscosity to the same degree as in the more globular cycloalkanes.

Our D values can also be compared with those obtained by others.^{33–35} Table 4 shows literature values for biphenyl in C₁₄ at 298.2 K³³ and biphenyl and anthracene in C₇ and C₈ at 303.2 K.³⁴ These data were obtained by Taylor dispersion methods, but the experimental setups including methods of sample introduction are different from ours. The agreement with values from our fits to eq 3 is good (the largest difference is 3.3%). Also shown in Table 4 are D values from delayed fluorescence studies of pyrene (in C₆) and anthracene (in C₆, C₈, and C₁₆) in their lowest triplet states at 298.2 K.³⁵ These excited-state values,

TABLE 5: Free Volume Parameters in the *n*-Alkanes at 25 °C

solute	<i>B</i>	$-(\ln A_{\text{FV}})$	p_{calcd}^a	p_{exptl}^b
O ₂ ^c	1.040 ± 0.018	7.559 ± 0.040	0.553	0.553
biphenyl	1.350 ± 0.023	8.782 ± 0.008	0.718	0.718
anthracene	1.440 ± 0.025	8.096 ± 0.056	0.766	0.749
diphenylacetylene	1.445 ± 0.021	8.173 ± 0.048	0.768	0.752
diphenylbutadiyne	1.530 ± 0.022	8.141 ± 0.051	0.814	0.797
pyrene	1.514 ± 0.026	8.069 ± 0.058	0.805	0.805
perylene	1.541 ± 0.031	8.164 ± 0.069	0.819	0.822
coronene	1.567 ± 0.057	8.245 ± 0.124	0.833	0.858
rubrene	1.811 ± 0.03	8.278 ± 0.060	0.963	0.943

^a From $p = B/B_\eta = B/1.881$. ^b From fits to eq 3. ^c From ref 10.

which are expected to be close to those for the ground state, are also in reasonable agreement with our values from eq 3 (the largest difference is 4.4%). Overall, the precision of our *D* values was reasonably good; the average uncertainty for all determinations of *D* for a given aromatic solute was 2.5% or less except for rubrene (3.22% in the *n*-alkanes, 3.79% in the cyclohexanes).³⁶ The uncertainties in *p* and log *A*_{SE} in Table 1 include these uncertainties in *D*.

Free Volume Approach. In ref 10, the *D* values for O₂ in C₆–C₁₆ at 25 °C were fitted to the Doolittle–Cohen–Turnbull free volume equation^{16,17}

$$D = A_{\text{FV}} \exp(-B/v_f) \quad (4)$$

where *A*_{FV} and *B* ≈ 1 are constants for a given solute–solvent system; the fractional free volume, *v*_f, is given in terms of the solvent's molar volume, *V*_m, and its zero-diffusion volume, *V*₀(*d*)¹⁶

$$v_f = [V_m - V_0(d)]/V_0(d) \quad (5)$$

The close-packing volume^{10,37} was used for *V*₀(*d*). Good linear correlations are also found for the aromatic hydrocarbons. The values of *B* and ln *A*_{FV} in Table 5 were obtained from fits to eqs 4 and 5 using *D* values calculated from eq 3 at 25 °C.³⁶

The free volume fit is related to that involving eq 3;^{10,38} the isothermal viscosities of the *n*-alkanes can be fitted using $\eta = A_\eta \exp(B_\eta/v_f)$ with *B*_η = 1.881 for C₆–C₁₆ at 25 °C (ln *A*_η = −8.809). Combining this eq for η with eq 4 gives $D\eta^p = A_{\text{SE}}A_\eta^p = \text{constant}$ with $p = B/B_\eta$; this is the isothermal version of eq 3. Table 5 shows that the experimental values of *p* are very close to those calculated using $p = B/B_\eta = B/1.881$. *B* (like *p*) generally increases as the solute size increases; this is consistent with Cohen and Turnbull's theory, in which *B* is the product of a geometric factor *g* (0.5 ≤ *g* ≤ 1) and the ratio $v^*/V_0(d)$, where *v*^{*} is a critical volume just large enough for diffusion to occur.^{17,39}

Comparison with Reorientational Results. Solvent-dependent reorientational data have been obtained for several of our solutes in the *n*-alkanes. When making comparisons with our translational results, eq 2 will be used in the form

$$1/D = (f\pi r/k_B)(\eta/T) \quad (6)$$

which, like the SED relation, is linear in η/T . Benzler and Luther⁵ used pump–probe polarization spectroscopy to study biphenyl in C₅–C₁₆. Their τ_θ values (Figure 5) show deviations from SED behavior, as do the translational results from the SE relation; the two sets of data have approximately the same dependence on η/T . Similar techniques were used by Jiang and Blanchard⁴ to determine τ_θ in both the ground and first excited

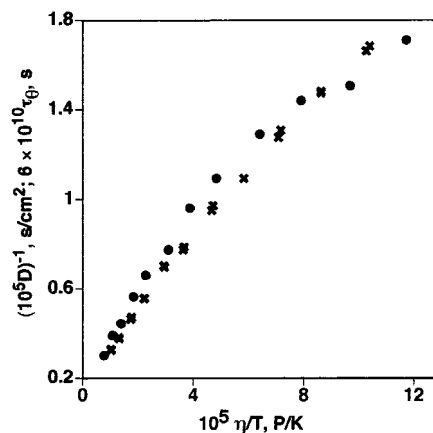


Figure 5. $(10^5 D)^{-1}$ (x) and $(6.0 \times 10^{10})\tau_\theta$ vs η/T (●) for biphenyl in the *n*-alkanes.

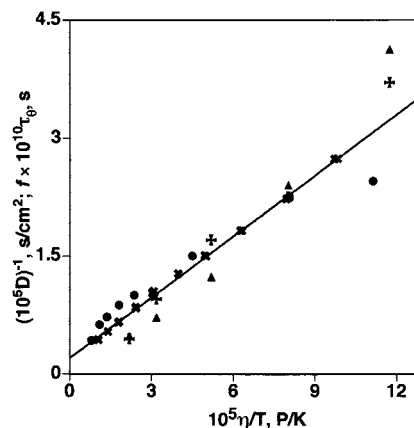


Figure 6. $(10^5 D)^{-1}$ (x) and $(f \times 10^{10})\tau_q$ vs η/T for perylene in the *n*-alkanes. $f = 5.0$ for one-photon excitation⁴ (●) and circularly polarized⁴⁰ two-photon excitation (▲); $f = 7.5$ for linearly-polarized⁴⁰ two-photon excitation (+). The straight line is a fit to the $(10^5 D)^{-1}$ data.

singlet states of perylene. They were the same within experimental accuracy; the average values, shown in Figure 6, have deviations from SE behavior. However, the τ_θ values in C₅–C₈ were found to be linear in η (at constant *T* = 300 K) as they were in C₉, C₁₀, C₁₂, and C₁₆;⁴ the slope for the shorter *n*-alkanes is larger than that for the longer solvents by a factor of 3. The difference in slopes was discussed⁴ in terms of a change in boundary conditions; the stick limit was more appropriate for C₅–C₈ while the slip limit was better for the longer solvents. The smaller slope in the longer solvents is also consistent with the solvent-dependent *r* values given in Table 3; i.e., the apparent “size” of perylene decreases as the chain length increases. Pauls et al.⁴⁰ determined τ_θ values (also shown in Figure 6) from anisotropy decays induced by two-photon excitation of perylene in C₉, C₁₀, C₁₂, C₁₄, and C₁₆. The slopes of plots of τ_θ vs η (at constant *T* = 290 K) for linear and circularly polarized excitation in their two-photon experiments gave essentially equal slopes that were larger than those found by Jiang and Blanchard⁴ for C₉, C₁₀, C₁₂, and C₁₆ in their single-photon studies (which had smaller uncertainties than the two-photon experiments).

When scaled for the purposes of comparison, the translational results roughly follow those for reorientation, although the $1/D$ data (Figure 6) appear to be linear in η/T . The apparent linearity is misleading; perylene has deviations from SE behavior with $p = 0.822 \pm 0.007$. These results indicate that eq 3 is more sensitive to deviations from Stokes–Einstein behavior than eq 6.

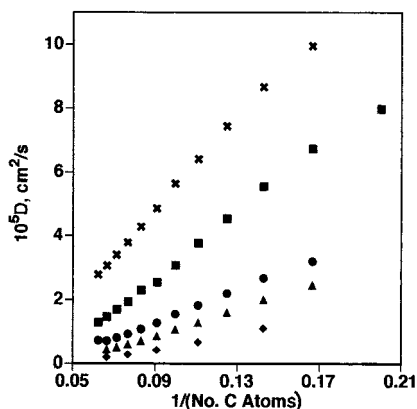


Figure 7. Diffusion constants vs $1/n$ in the n -alkanes for O_2 (\times), ^{133}Xe (\blacksquare), biphenyl (\bullet), perylene (\blacktriangle), and rubrene (\blacklozenge). Except for ^{133}Xe (20 °C),³⁸ the D values are at 25 °C from the fits to eq 3.

The differences in the dependence of τ_θ and $1/D$ on η/T for perylene and, to some extent, biphenyl may arise because the induced orientational anisotropy function⁴ (from which τ_θ is determined) and D are different functions of the principal values of the rotational and translational diffusion tensors, respectively. There could be axis-dependent solute-solvent interactions. The reorientational and translational motions also can have different dependencies on the solute-solvent interactions. Pauls et al.⁴⁰ noted that the anisotropy decays induced by one- and two-photon excitation are different functions of the rotational diffusion tensor elements.

In related studies, Hochstrasser et al.⁶ used picosecond polarization spectroscopy to determine reorientational correlation times for *trans*-stilbene and (*E,E*)-ditetrahydronaphthylideneethane (stiff diphenylbutadiene) in C_5 – C_{16} . The constant-temperature τ_θ values showed deviations from SE behavior similar to those for biphenyl; they were more pronounced for the smaller *trans*-stilbene. Kim and Fleming⁷ found similar deviations for *trans*-stilbene at constant temperature in C_5 , C_6 , C_8 , C_{10} , C_{12} , C_{14} , and C_{16} ($\tau_\theta \approx \eta^{0.7}$). The temperature-dependent data in the individual solvents were linear in η/T , but the slopes decreased as the solvent chain length increased. This too is consistent with an apparent decrease in the solute volume as the solvent chain length increases.

Comparison with MD Results. van der Vegt and co-workers⁴¹ calculated the diffusion constant of a small molecule, CH_4 , in n -alkane liquids; the dependence on n , the number of solvent carbon atoms, was found to be $D \approx n^{-\alpha}$ with $\alpha = 1.0 \pm 0.1$. Figure 7 shows the n -alkane data for O_2 , ^{133}Xe ,⁴² biphenyl, perylene, and rubrene. As seen previously,¹⁰ the D values for O_2 and ^{133}Xe are approximately linear in n^{-1} . The correlation appears to be less successful for the larger biphenyl, perylene, and rubrene.

Summary and Conclusions

The translational diffusion constants of several solutes have been determined using capillary flow techniques.^{9,10} Biphenyl, diphenylacetylene, diphenylbutadiene, anthracene, pyrene, rubrene, perylene, and coronene were studied in the n -alkanes. Pyrene and rubrene were also studied in cyclohexane and three of its derivatives. The results are compared with those found previously for O_2 in the n -alkanes and cycloalkanes.

Deviations from the SE relation, eq 2, have been found; for all but one of the solute-solvent systems, the solute size decreases as the solvent viscosity increases. The data can be fitted to eq 3, in which values of $p < 1$ indicate deviations from

SE behavior ($p = 1$). In both the n -alkanes and cycloalkanes, the value of p increases as the solute size increases; when a given solute is studied in both types of solvent, the p value is always larger in the cycloalkanes. The smallest p values are found for O_2 (0.553 ± 0.009 in the n -alkanes, 0.632 ± 0.017 in the cycloalkanes), and the largest are found for rubrene (0.943 ± 0.014 in the n -alkanes, 0.982 ± 0.019 in the cycloalkanes).

The dependence of $1/D$ on η/T for several of our solutes is approximately the same as that of τ_θ , the reorientational correlation time. The D values are also compared with the results of MD calculations⁴¹ and have been fitted to the Doolittle-Cohen-Turnbull^{16,17} free volume equation. A correlation between the p values and the results of the free volume analyses is discussed.

Acknowledgment. The Department of Chemistry, Saint Louis University, has supported this research. The data acquisition system and detector were purchased with grants to Dr. Barry Hogan from Research Corp. and the donors of the Petroleum Research Fund, administered by the American Chemical Society.

References and Notes

- Deppe, D. D.; Miller, R. D.; Torkelson, J. M. *J. Polym. Sci., B: Polym. Phys.* **1996**, *34*, 2987.
- Korolev, V. V.; Bolotsky, V. V.; Shokhirev, N. V.; Krissinel, E. B.; Bagryansky, V. A.; Bazhin, N. M. *Chem. Phys.* **1995**, *196*, 317.
- Engelke, M.; Behmann, T.; Ojeda, F.; Diehl, H. A. *Chem. Phys. Lipids* **1994**, *72*, 35.
- Jiang, Y.; Blanchard, G. J. *J. Phys. Chem.* **1994**, *98*, 6436.
- Benzler, J.; Luther, K. *Chem. Phys. Lett.* **1997**, *279*, 333.
- Lee, M.; Bain, A. J.; McCarthy, P. J.; Han, C. H.; Haseltine, J. N.; Smith, A. B., III; Hochstrasser, R. M. *J. Chem. Phys.* **1986**, *85*, 4341.
- Kim, S. K.; Fleming, G. R. *J. Phys. Chem.* **1988**, *92*, 2168.
- Equation 1 is often written with a zero-viscosity intercept, τ_0 ; see refs 5 and 6 and Evans, G. T.; Kivelson, D. *J. Chem. Phys.* **1986**, *84*, 385.
- Kowert, B. A.; Dang, N. C. *J. Phys. Chem. A* **1999**, *103*, 779.
- Kowert, B. A.; Dang, N. C.; Reed, J. P.; Sobush, K. T.; Seele, L. G., III. *J. Phys. Chem. A* **2000**, *104*, 8823.
- Pollack, G. L.; Kennan, R. P.; Himm, J. F.; Stump, D. R. *J. Chem. Phys.* **1990**, *92*, 625.
- Bello, M. S.; Rezzonico, R.; Righetti, P. G. *Science* **1994**, *266*, 773.
- Grushka, E.; Levin, S. In *Quantitative Analysis Using Chromatographic Techniques*; Katz, E., Ed.; Wiley: Chichester, U.K., 1987; p 359.
- Pollack, G. L.; Enyeart, J. J. *Phys. Rev. A* **1985**, *31*, 980.
- Chen, S.-H.; Davis, H. T.; Evans, D. F. *J. Chem. Phys.* **1982**, *77*, 2540.
- Doolittle, A. K. *J. Appl. Phys.* **1952**, *23*, 236.
- Cohen, M. H.; Turnbull, D. *J. Chem. Phys.* **1959**, *31*, 1164.
- Viswanath, D. S.; Natarajan, G. *Data Book on the Viscosity of Liquids*; Hemisphere Publishing: New York, 1989.
- Andrussow, L.; Schramm, B. *Landolt-Bernstein Zahlenwerte und Funktionen*, 6th ed.; Springer-Verlag: New York, 1969.
- Cowan, D. O.; Drisko, R. L. *Elements of Organic Photochemistry*; Plenum Press: New York, 1978.
- Nardello, V.; Marti, M.-J.; Pierlot, C.; Aubry, J.-M. *J. Chem. Educ.* **1999**, *76*, 1285.
- Huhey, J. E.; Keiter, E. A.; Keiter, R. L. *Inorganic Chemistry*, 4th ed.; HarperCollins: New York, 1993.
- Hargreaves, A.; Rizvi, S. H. *Acta Crystallogr.* **1962**, *15*, 365.
- Almeningen, A.; Bastiansen, O. *K. Nor. Vidensk. Selsk., Skr.* **1958**, No. 4.
- Abramenkov, A. V.; Almeningen, A.; Cyvin, B. N.; Cyvin, S. J.; Jonvik, T.; Khaikin, L. S.; Romming, C.; Vikov, L. V. *Acta Chem. Scand., A* **1988**, *42*, 674.
- Coates, G. W.; Dunn, A. R.; Henling, L. M.; Dougherty, D. A.; Grubbs, R. H. *Angew. Chem., Int. Ed. Engl.* **1997**, *36*, 248.
- Salem, L. *Molecular Orbital Theory of Conjugated Systems*; W. A. Benjamin, Inc.: New York, 1966.
- Camerman, A.; Trotter, J. *Acta Crystallogr.* **1965**, *18*, 636.
- Campbell, R. A.; Robertson, J. M.; Trotter, J. *Acta Crystallogr.* **1962**, *15*, 289.
- Camerman, A.; Trotter, J. *Proc. R. Soc. London, A* **1964**, *279*, 129.
- Bondi, A. *J. Phys. Chem.* **1964**, *68*, 441.

- (32) Venable, R. M.; Zhang, Y.; Hardy, B. J.; Pastor, R. W. *Science* **1993**, *262*, 223.
- (33) Chan, T. C.; Chan, M. L. *J. Chem. Soc., Faraday Trans.* **1992**, *88*, 2371.
- (34) Fan, Y.; Qian, R.; Cheng, M.; Shi, M.; Shi, J. *Ber. Bunsen-Ges. Phys. Chem.* **1995**, *99*, 1043.
- (35) Meyer, E. G.; Nickel, B. *Z. Naturforsch., A* **1980**, *35*, 503.
- (36) The uncertainties in p for pyrene (± 0.006) and rubrene (± 0.014) in the n -alkanes in Table 1 are slightly larger than those given in ref 10 (± 0.005 and ± 0.008 for pyrene and rubrene, respectively), which did not include the uncertainties in D . The uncertainties for B and $-(\ln A_{FV})$ in Table 5 were obtained using values of D calculated from eq 3 and only reflect the uncertainties in the fit to eqs 4 and 5.

- (37) Dymond, J. H.; Assael, M. J. In *Transport Properties of Fluids*; Millat, J., Dymond, J. H., Nieto de Castro, C. A., Eds.; Cambridge University Press: Cambridge, U. K, 1996; p 226.
- (38) Gavish, B.; Yedgar, S. In *Protein-Solvent Interactions*; Gregory, R. B., Ed.; Marcel Dekker: New York, 1995; p 343.
- (39) Cook, R. L.; King, H. E., Jr.; Herbst, C. A.; Herschbach, D. R. *J. Chem. Phys.* **1994**, *100*, 5178.
- (40) Pauls, S. W.; Hedstrom, J. F.; Johnson, C. K. *Chem. Phys.* **1998**, *237*, 205.
- (41) van der Vegt, N. F. A.; Briels, W. J.; Wessling, M.; Strathmann, H. *J. Chem. Phys.* **1998**, *108*, 9558.
- (42) Pollack, G. L.; Enyeart, J. J. *Phys. Rev. A* **1985**, *31*, 980.